Nanoscale

Accepted Manuscript

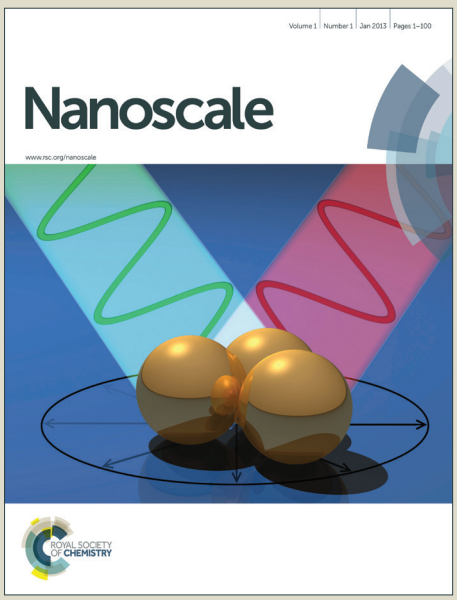

ROYAL SOCIETY OF CHEMISTRY

www.rsc.org/nanoscale

Journal Name

RSCPublishing

ARTICLE

Immobilizing water-soluble graphene quantum dots with gold nanoparticles for low potential electrochemiluminescence immunosensor

Cite this: DOI: 10.1039/x0xx00000x

Received 00th March 2015
Accepted 00th March 2015

DOI: 10.1039/x0xx00000x

www.rsc.org/

Yongqiang Dong, Huan Wu, Pengxiang Shang, Xiaoting Zeng, and Yuwu Chi*

Hydrazide-modified graphene quantum dots (HM-GQDs) obtained by refluxing GQDs with hydrazine hydrate were hybridized with gold nanoparticles (AuNPs) through the redox reaction between HM-GQDs and $AuCl_4^-$. The obtained nano-hybrids (HM-GQDs-AuNPs) possess the unique electrochemiluminescence (ECL) properties of HM-GQDs and the easy self-assembly with some bio-molecules of AuNPs, which have great potential applications in bio-sensors. HM-GQDs-AuNPs were modified on a glassy carbon electrode to develop a novel ECL immunosensor of carcinoembryonic antigen (CEA) as a model target analyte. Due to the increment of electron-transfer resistance after immunoreaction, the ECL intensity decreased as the concentration of CEA was increased. The linear response range was between 0.02 and 80 $ng \cdot mL^{-1}$, and the detection limit was 0.01 $ng \cdot mL^{-1}$.

1 Introduction

Carbon based dots (CDs) are emerging luminescent nanomaterials, which exhibit unique optical properties, such as photoluminescence (PL), chemiluminescence (CL) and electrochemiluminescence (ECL).[1, 2] Furthermore, CDs present many advantages over traditional semiconductor-based quantum dots (QDs), such as robust chemical inertness, low toxicity, easy preparation and low cost.[3] Accordingly, CDs are considered to have great potential applications in many field, including bio-imaging,[4, 5] bio-sensing,[6, 7] and environmental analysis.[8-10] However, most of the applications about CDs are based on their PL properties, while much less attention has been paid to the ECL sensors of CDs. ECL is a powerful analytical technique. Combining the advantages of CL and electrochemical analysis, ECL analysis shows many advantages over the FL analysis, such as wide response range and high sensitivity.[11, 12] Since the ECL properties of CDs was first reported in 2009,[13] increasing attention has been focused on the unique properties of CDs.[14-18] Furthermore, some chemical sensors and bio-sensors have been developed based on the strong cathodic ECL of CDs.[14-16, 19, 20] However, most CDs emit strong cathodic ECL signal only at rather negative potential region, such as -1.50 V,[13-17, 19-21] where water molecules can be electrolyzed. where water molecules can be electrolyzed. The electrogenerated large quantities of hydrogen bubbles from water molecules will interfere greatly the ECL detection if using disk electrodes, and may destroy sensing membranes at the electrode surfaces. Apparently, the sensing applications based on the cathodic ECL of CDs would be greatly limited. Recently, we have synthesized hydrazide-modified graphene quantum dots (HM-GQDs), which exhibit excellent PL, CL, and especially the anodic ECL activities at low potential due to the contained luminol-like units.[22] Accordingly, HM-GQDs would have great potential applications in sensing, especially bio-sensing. However, it would be difficult to apply directly HM-GQDs in bio-sensing. First of all, the good solubility made HM-GQDs difficult to be immobilized on the surfaces of electrodes. Secondly, HM-GQDs might need a boring bio-labelling before being applied in bio-sensing. Herein, HM-GQDs would be hybridized with gold nanoparticles (AuNPs), which have been widely applied in many fields due to their unique optoelectronic properties.[23, 24] In particular, the excellent biocompatibility and ease of functionalization make them an effective platform for the fabrication of label-free biosensors.[25] Therefore, AuNPs might be ideal carriers to immobilize the soluble HM-GQDs. In this paper, HM-GQDs were hybridized with AuNPs by reducing $HAuCl_4$ with HM-GQDs. The obtained nano-hybrids (HM-GQDs-AuNPs) can be modified easily on the surfaces of glassy carbon electrodes (GCE), and exhibit strong anodic ECL activity in the presence of H_2O_2. To investigate the potential applications of HM-GQDs-AuNPs in bio-sensing, carcinoembryonic antigen (CEA), which can be used as a tumor marker in clinical tests,[26] was chosen as a model target analyte. The easy procedure and satisfactory results suggest the promising applications of HM-GQDs-AuNPs in clinical immunoassay.

2 Experimental

2.1 Materials

Hydrogen tetrachloroaurate trihydrate ($HAuCl_4 \cdot 3H_2O$), L-cysteine (L-Cys) and L-glutamate (L-Glu) were purchased from Sigma-Aldrich. Hydrogen peroxide (H_2O_2) and hydrazine hydrate (N_2H_4) were obtained from Fuchen Chemical Reagent Co. (Tianjin, China). Vulcan XC-72 carbon black was purchased from Cabot Corporation (USA). Bovine serum (BSA, >98.0%) was from Sangon Biotech Co. (Shanghai, China). Carcinoembryonic antibody (Anti-CEA), alphafetoproten (AFP), luteotropic hormone (LH) and human IgG (HIgG), were obtained from Biocell Biotechnol. Co., Ltd. (Zhengzhou, China). All other reagents were of analytical reagent grade and used without further purification. 0.1 M phosphate buffer solution (PBS) of various pH was prepared by mixing appropriate volumes of 0.1 M H_3PO_4 and 5 M NaOH

Journal Name RSCPublishing

ARTICLE

Scheme 1. (A) Schematic illustration of preparation of HM-GQDs-AuNPs and (B) the proposed ECL immunosensor.

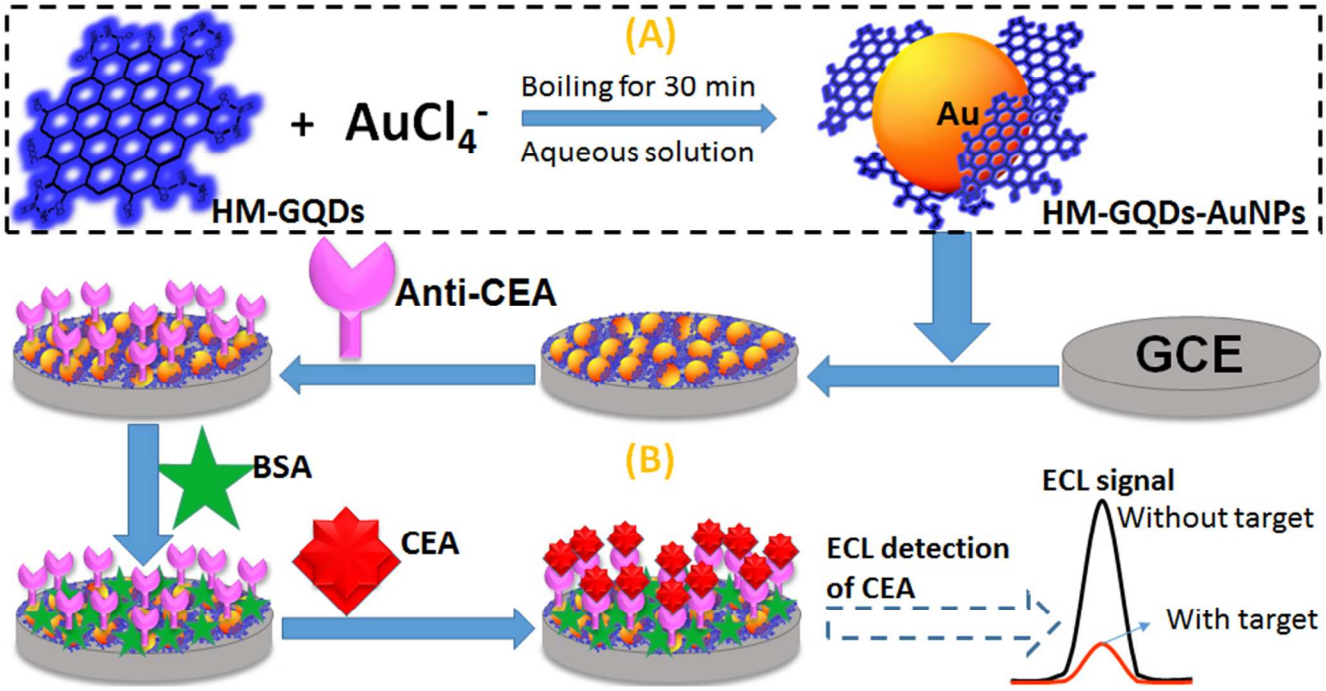

stock solutions. Doubly distilled water was used throughout this work.

2.2 Synthesis of GQDs

GQDs were prepared by a chemical oxidation method according to a previous work.[27] In brief, 2 g XC-72 carbon black was refluxed with 250 mL 8 M HNO_3 at 130 °C for 24 h. After a natural cooling and a centrifugation (2770g for 10 min), the supernatant was collected and dried at 150 °C to obtain orange powder (GQDs).

2.3 Synthesis of HM-GQDs

HM-GQDs were synthesized by refluxing GQDs with N_2H_4 following a previously report method.[20] In brief, the mixture of 100 mL 2.5 mg /mL GQDs solution and 2mL N_2H_4 was refluxed at 65 °C for 24 h. After the reaction, the solution was cooled to room temperature and dried under vacuum to remove water and the redundant N_2H_4. Finally, some black HM-GQDs powder was obtained.

2.4 Synthesis of HM-GQDs-AuNPs

Gold colloids were prepared by the reduction of $HAuCl_4$ with HM-GQDs (see Scheme 1a). In a typical procedure, 1mL $HAuCl_4$ solution (0.5%, w/w) was added rapidly into 50 mL boiling HM-GQDs solution (0.02%, w/w) under stirring. The solution was kept boiling for 30 min. Then the heating source was removed, and the solution was cooled naturally to room temperature while the stirring was continued. Finally, the mixture was centrifuged at 16500g for 10 min for 5 times. The precipitate was redispersed in doubly distilled water and stored at 4 °C.

2.5 Fabrication of ECL immunosensor

First, 5 μL of the as-prepared HM-GQDs-AuNPs suspension (1.2 mg/mL) was dropped onto the polished GCE (2 mm in diameter). After being dried naturally, the modified electrode was washed with PBST (10 mM, pH 7.4 PBS containing 0.05% Tween-20) to remove free HM-GQDs-AuNPs. The GCE/HM-GQDs-AuNPs was obtained when the electrode was dried naturally. Second, 5 μL anti-CEA solution (in 10 mM, pH 6.0 PBS) was dropped on the surface of GCE/HM-GQDs-AuNPs and dried naturally. The modified electrode was washed thoroughly with PBST to remove physically absorbed anti-CEA, and dried to obtain GCE/HM-GQDs-AuNPs/anti-CEA. Third, 5 μL BSA solution (2%) was dropped on the surface of the modified electrode to prevent non-specific adsorption by blocking the potential active binding sites for protein. The obtained modified electrode was labeled as GCE/HM-GQDs-AuNPs/anti-CEA/BSA. After the modified electrode was washed thoroughly with PBST and dried naturally, 5 μL target CEA sample was dropped on the modified electrode and dried naturally. After carefully washing the electrode with PBST, the ECL signal of the immunosensor was detected in pH 9.0 PBS.

2.6 Instrumentation

High-resolution transmission electron microscopy (HRTEM) measurements were performed on an electronic microscope (Tecnai

G2 F20S-TWIN). The height distribution of the obtained HM-GQDs-AuNPs was characterized by an atomic force microscope (AFM) (Nanoman, Veeco, Santa Barbara, CA) with tapping mode. The crystal structure of HM-GQDs-AuNPs was characterized by X-ray diffraction (XRD) by a Bruker AXS diffractometer (l ¼ 0.15418 nm). X-Ray photoelectron spectroscopy (XPS) data was measured by a Kratos AXIS Ultra spectrometer with a monochromatized Al Ka X-ray source (1486.71 eV) for determining the composition and chemical bonding configurations. UV/vis spectra were characterized by a UV/vis spectrophotometer (Lambda 750). The Fourier transform infrared (FTIR) spectrum of dried GQDs was obtained on a FT-IR spectrophotometer (Thermo Nicolet 360). Electrochemical (EC) and ECL measurements were carried out on an ECL detection system (MPI-E, Remex Electronic Instrument Lt. Co., Xi'an, China) equipped with a three-system (a modified GCE, a Pt wire counter electrode and a Ag/AgCl reference electrode containing 3 M KCl solution). Electrochemical impedance spectroscopy (EIS) detections were carried out on an AutoLab μAUTIII.FRA2.v electrochemical workstation (Eco Chemie, The Netherlands) in the solution of 0.1 M KNO_3 containing 20 mM $K_3[Fe(CN)_6]/K_4[Fe(CN)_6]$.

3 Results and discussion

3.1 Characterization of HM-GQDs-AuNPs

As shown in Figure 1A, HM-GQDs are nano-sheets of about 5 nm in lateral size. Well-defined lattice fringes with spacing of 0.21 nm can be observed, corresponding to the (100) facet of graphite (Figure S1). Most HM-GQDs are well-dispersed in the aqueous solution due to the abundant functional groups, such as hydroxyl group, carboxyl group and hydrazide group. After being refluxed with $HAuCl_4$, the reductive groups on HM-GQDs such as hydroxyl group and hydrazide group can reduce $HAuCl_4$ into AuNPs. At the same time, the well-dispersed HM-GQDs aggregate slightly, which may be due to the reaction between the residual amino groups and the carboxyl group. Furthermore, the residual functional groups of HM-GQDs combine the formed AuNPs, leading to the formation of HM-GQDs-AuNPs nano-hybrids. Figure 1B shows the TEM image of the obtained HM-GQDs-AuNPs. AuNPs of 10 to 30 nm in size without regular morphologies were distributed uniformly on the aggregated HM-GQDs. The AFM image (Figure S3) indicates that the heights of HM-GQDs-AuNPs distribute mainly 10 to 30 nm, indicating that the height on the obtained HM-GQDs-AuNPs should be mainly dependent on the size of AuNPs. The Raman spectrum of HM-GQDs-AuNPs shows obvious G band and D band of HM-GQDs at 1365 and 1605 cm^{-1}, respectively. XRD pattern of the obtained HM-GQDs-AuNPs (Figure S4) shows a broad (002) peak for the HM-GQDs and four diffraction peaks at 2θ degrees of 38.2, 44.4, 64.8 and 77.5, which are assigned to face-centered cubic (fcc) Au (111), (200), (220) and (311), respectively.[28] XPS spectrum illustrates that the obtained HM-GQDs-AuNPs are mainly compose of carbon, oxygen, nitrogen and gold elements (Figure S5). The results confirm that AuNPs have been successfully hybridized with HM-GQDs.

The high resolution C1s spectra (Figure S6) reveal the presence of sp^2 C-C, C-N, C-O and O=C-OH groups, which is quite similar with those of HM-GQDs.[20] Comparing the FTIR spectrum of HM-GQDs-AuNPs with that of HM-GQDs (see Figure 1C), the relative intensities of C=O and $–NO_2$ groups increased obviously while that of –OH decreased, implying that the reductive functional groups of HM-GQDs have been partially oxidized by $HAuCl_4$. However, the intense absorption bands of N-H and C-N groups suggest that a large quantity of residual luminol-like units present on HM-GQDs-AuNPs. Furthermore, the abundant oxygen-containing groups

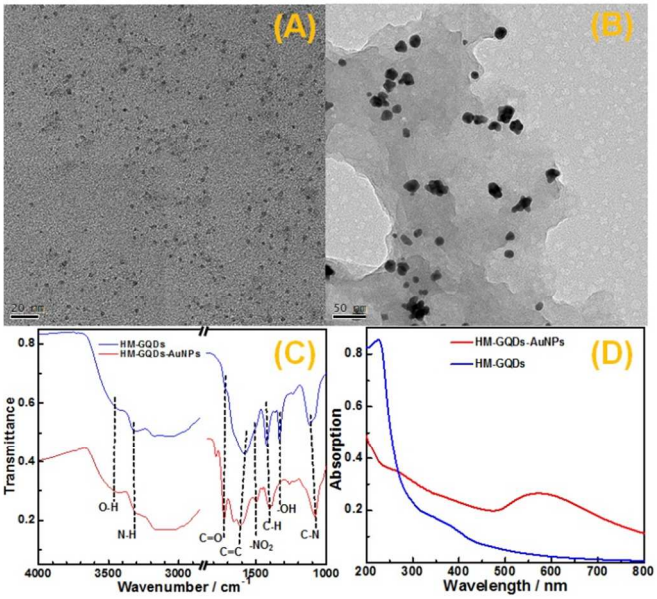

Fig. 1 (A) TEM image of HM-GQDs; (B) TEM image of HM-GQDs-AuNPs; (C) FTIR spectra of HM-GQDs and HM-GQDs-AuNPs; (D) UV-vis absorption spectra of HM-GQDs and HM-GQDs-AuNPs.

make the obtained HM-GQDs-AuNPs can be well dispersed in aqueous solution. Figure 1D shows the UV-vis absorption spectra of HM-GQDs and HM-GQDs-AuNPs. A characteristic absorption peak of AuNPs centered at around 570 nm can be observed from the UV-vis absorption spectrum of HM-GQDs-AuNPs, further confirming the formation of AuNPs. Besides that, a characteristic absorption band of HM-GQDs centered at around 385 nm, which should be caused by their contained luminol-like units,[19] can be also observed from the UV-vis absorption spectrum of HM-GQDs-AuNPs. It should be mentioned that the background absorption of HM-GQDs-AuNPs are much more obvious than that of HM-GQDs, which may be attributed to the aggregated HM-GQDs. The results further confirm the presence of the abundant residual luminol-like units on HM-GQDs-AuNPs. That is to say, HM-GQDs-AuNPs should have similar anodic ECL behaviors like HM-GQDs.

3.2 ECL behaviors of HM-GQDs-AuNPs.

HM-GQDs-AuNPs were modified on a freshly polished GCE to investigate their electrochemical and ECL behaviors (Figure 2A). Compared with bare GCE, GCE/HM-GQDs-AuNPs shows an obvious anodic wave with a peak at around +0.60 V. Correspondingly, an anodic ECL signal of GCE/HM-GQDs-AuNPs can be detected at potential higher than +0.40 V. Furthermore, the anodic ECL signal can be enhanced greatly by H_2O_2. As shown in Figure 2B, the ECL intensity increases linearly with the concentration of H_2O_2 below 1 mM, then increases slightly when the concentration of H_2O_2 is further increased to 1.5 mM, and finally has no obvious increase when the concentration of H_2O_2 is higher than 1.5 mM. The ECL intensity of GCE/HM-GQDs-AuNPs in the presence of H_2O_2 is dependent seriously on the pH value of solution. As shown in Figure 2C, the nano-hybrids show ECL activity in a wide pH range, i.e. pH 6-11. The ECL intensity increases with the pH value below pH 9,

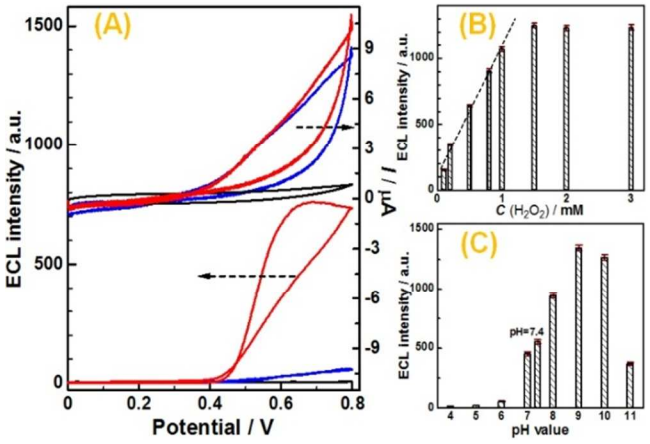

Fig. 2 (A) Cyclic voltammograms (Upper lines) and ECL emission curves (Lower lines) of bare GCE (black lines), GCE/HM-GQDs-AuNPs in the absence (blue lines) and presence of 0.5 mM H_2O_2 at pH 9.0; (B) Effect of the concentration of H_2O_2 on the ECL intensity of GCE/HM-GQDs-AuNPs in pH 9 PBS; (C) Effect of pH value on the ECL intensity of GCE/HM-GQDs-AuNPs in the presence of 1.5 mM H_2O_2. Scan rate: 0.1 V/S.

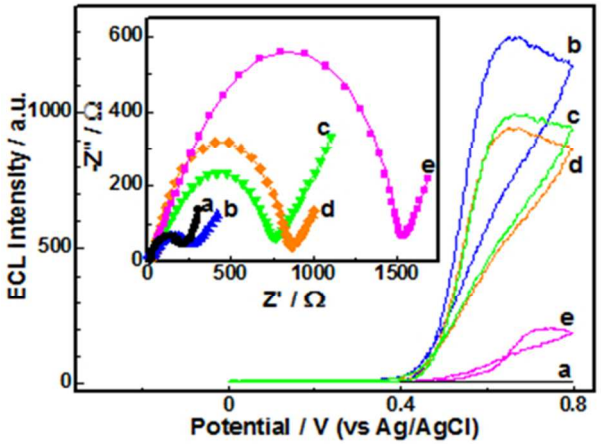

Fig. 3 ECL responses of bare GCE (a), GCE/HM-GQDs-AuNPs (b), GCE/HM-GQDs-AuNPs/anti-CEA (c), GCE/HM-GQDs-AuNPs/anti-CEA/BSA (d) and GCE/HM-GQDs-AuNPs/anti-CEA/BSA/CEA(e) at the CEA concentration of 20 ng· mL^{-1}. Inset shows the corresponding EIS in 0.1 M KNO_3 containing 20.0 mM $K_3[Fe(CN)_6]/K_4[Fe(CN)_6]$. Scan rate: 0.1 V/S.

and reaches the maximum at pH 9, then decreases when the pH value is further increased. The pH-dependent ECL intensity of GCE/HM-GQDs-AuNPs in the presence of H_2O_2 should be mainly related to the ECL activities of HM-GQDs at different pH value.[20] Apparently, the hybridization with AuNPs has no obvious effect on the ECL properties of HM-GQDs. These results indicate that AuNPs are ideal candidates to hybridize HM-GQDs, making HM-GQDs easy to be immobilized on the surface of electrode without obvious change in ECL activities. It should be pointed out that the nano-hybrids also exhibit good ECL activity at physiological pH (7.4), suggesting the great potential applications of the nano-hybrids in biosensing.

Based on above mentioned experimental results, pH 9 PBS containing 1.5 mM H_2O_2 was used as the ECL reaction solution to get the highest immunosensing sensitivity.

3.3 ECL Immunosensor based on HM-GQDs-AuNPs

As shown in Scheme 1B, a strategy has been proposed to develop ECL immunosensor based on HM-GQDs-AuNPs. To characterize the fabrication process of the ECL immunosensor, ECL signals of each immobilization steps were detected (see Figure 3). GCE/HM-GQDs-AuNPs exhibit strong anodic ECL signal, which is quenched gradually as anti-CEA, BSA and CEA is progressively conjugated. It has been well discussed that the ECL decrease in such type of immunosensors should be attributed to the increased electron-transfer resistance, Ret, in reaction.[29, 30] As an effective method for probing the features of surface-modified electrodes, EIS was employed to characterize the surface features of the modified electrode at different stages (see the inset of Figure 3). The gradual increase in the diameter of semicircle implies that Ret is increasing through the immobilization of HM-GQDs-AuNPs, anti-CEA, BSA, and CEA. Apparently, the EIS results are consistent well with the ECL results, confirming that the ECL quenching should be attributed to the increased Ret caused by the immobilized insulating layers.

The linear response range of the immunosensor was measured. As shown in Figure 4A, the ECL intensity (the average value from 10 parallel measurements) decreased gradually with increasing the concentration of CEA. The standard calibration curve for the CEA detection is shown in the inset of Figure 4A. A good semilogarithmic correlation can be observed between the quenched ECL intensity and the concentration of CEA in the range from 0.02 to 80 ng· mL^{-1}.

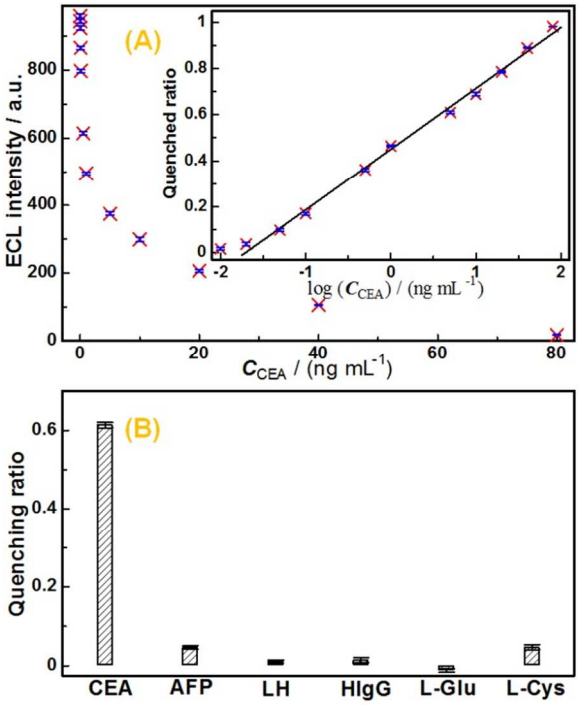

Fig. 4 (A) Calibration curve for CEA determination. Inset shows the linear plot of the quenched ECL intensity vs logarithmic concentration of CEA. (B) Specificity of the immunosensor towards CEA (data was the average of five parallel tests).

The detection limit is 0.01 ng· mL^{-1} at a signal-to-noise ratio of 3. These results are comparable with those of other reported methods.[31-33] To evaluate the specificity, ECL responses of the immunosensor towards five other bio-molecules, AFP, LH, HIgG, L-Cys and L-Glu, that may interfere the detection of CEA were also investigated. It can be observed from Figure 4B, the target CEA produces significantly higher ECL response than the other bio-molecules, indicating the high specificity of the ECL immunosensor.

4 Conclusions

The new nano-hybrids, HM-GQDs-AuNPs, were synthesized through a direct redox reaction between HM-GQDs and $AuCl_4^-$. HM-GQDs-AuNPs were immobilized easily on the surface of GCE, and exhibited excellent anodic ECL activities at low potential below +0.80 V. In the presence of H_2O_2, HM-GQDs-AuNPs modified GCE emitted strong ECL signal in neutral and weak alkaline solutions. Based on the unique ECL behavior of HM-GQDs-AuNPs, a novel label-free ECL immunosensor for the rapid, sensitive detection of GCE was developed. This research opens new avenues to apply the ECL properties of CDs in analytical systems and biosensors.

Acknowledgements

This study was financially supported by National Natural Science Foundation of China (21375020, 21305017), National Basic Research Program of China (2010CB732400), and the Program for Changjiang Scholars and Innovative Research Team in University (No. IRT1116).

Notes and references

The authors declare no competing financial interest.

Ministry of Education Key Laboratory of Analysis and Detection Technology for Food Safety, Fujian Provincial Key Laboratory of Analysis and Detection Technology for Food Safety, and Department of Chemistry, Fuzhou University, Fujian 350108, China. Fax: +86-591-22866137; Tel: +86-591-22866137; E-mail: y.w.chi@fzu.edu.cn

1. H. Sun, L. Wu, W. Wei, X. Qu, *Mater. Today,* 2013, **16**, 433−442.
2. Z. Zhang, J. Zhang, N. Chen, L. Qu, *Energy Environ. Sci.,* 2012, **5**, 8869−8890.
3. J. Shen, Y. Zhu, X. Yang, C. Li, *Chem. Commun.,* 2012, **48**, 3686–3699.
4. S. Yang, L. Cao, P. G. Luo, F. Lu, X. Wang, H. Wang, M. J. Meziani, Y. Liu, G. Qi, Y. Sun, *J. Am. Chem. Soc.,* 2009, **131**, 11308−11309.
5. M. Nurunnabi, Z. Khatun, K. M. Huh, S. Y. Park, D. Y. Lee, K. J. Cho, Y. Lee, *ACS Nano,* 2013, **7**, 6858–6867.
6. Y. Wang, L. Zhang, R. Liang, J. Bai, J. Qiu, *Anal. Chem.,* 2013, **85**, 9148−9155.
7. P. Shen, Y. Xia, *Anal. Chem.,* 2014, **86**, 5323−5329.
8. Y. Dong, R. Wang, G. Li, C. Chen, Y. Chi, G. Chen, *Anal. Chem.,* 2012, **84**, 6220−6224.
9. Y. Dong, G. Li, N. Zhou, R. Wang, Y. Chi, G. Chen, *Anal. Chem.,* 2012, **84**, 8378–8382.
10. X. Liu, N. Zhang, T. Bing, D. Shangguan, *Anal. Chem.,* 2014, **86**, 2289−2296.
11. B. Yin, S. Dong, E. Wang, *Trends Anal. Chem.,* 2004, **23**, 432–438.
12. R. D. Gerardi, N. W. Barnett, S. W. Lewis, *Anal. Chim. Acta,* 1999, **378**, 1–4.
13. L. Zheng, Y. Chi, Y. Dong, J. Lin, B. Wang, *J. Am. Chem. Soc.,* 2009, **131**, 4564–4565.
14. L. Li, J. Ji, R. Fei, C. Wang, Q. Lu, J. Zhang, L. Jiang, J. Zhu, *Adv. Funct. Mater.,* 2012, **22**, 2971−2979.
15. Y. Dong, W. Tian, S. Ren, R. Dai, Y. Chi, G. Chen, *ACS Appl. Mater. Interfaces,* 2014, **6**, 1646−1651.
16. Y. Chen, Y. Dong, H. Wu, C. Chen, Y. Chi, G. Chen, *Electrochim. Acta,* 2015, **56**, 552–557.
17. Y. Dong, C. Chen, J. Lin, N. Zhou, Y. Chi, G. Chen, *Carbon,* 2013, **56**, 12−17.
18. H. Zhu, X. Wang, Y. Li, Z. Wang, F. Yang, X. Yang, *Chem. Commun.,* 2009, **34**, 5118−5120.
19. L. Wu, J. Wang, J. Ren, W. Li, X. Qu, *Chem. Commun.,* 2013, **49**, 5675−5677.
20. M. Zhang, H. Liu, L. Chen, M. Yan, L. Ge, S. Ge, J. Yu, *Bio. Bio.*, 2013, **49**, 79−85.
21. Y. Xu, M. Wu, X. Feng, X. Yin, X. He, Y. Zhang, *Chem. Eur. J.* 2013, **19**, 6282−6288.
22. Y. Dong, R. Dai, T. Dong, Y. Chi, G. Chen, *Nanoscale*, 2014, **6**, 11240−11245.
23. D. A. M.C. Daniel, *Chem. Rev.*, 2004, 104, 293−346.
24. W. Zhao, M. A. Brook, Y. Li, *Chembiochem.*, 2008, **9**, 2363−2371.
25. R. A. Sperling, G. P. Rivera, F. Zhang, M. Zanella, W. J. Parak, *Chem. Soc. Rev.*, 2008, **37**, 1896–1908.
26. S. Benchimol, A. Fuks, S. Jothy, N. Beauchemin, K. Shirota, C. P. Stanners, *Cell*, 1989, **57**, 327–334.
27. Y. Dong, C. Chen, X. Zheng, L. Gao, Z. Cui, H. Yang, C. Guo, Y. Chi, C. M. Li, *J. Mater. Chem.*, 2012, **22**, 8764–8766.
28. H. Zhang, J. J. Xu, H. Y. Chen, *J. Phys. Chem. C*, 2008, 112, 13886–13892.
29. G. Jie, J. Zhang, D. Wang, C. Cheng, H. Chen, J. Zhu, *Anal. Chem.*, 2008, **80**, 4033–4039.
30. G. Jie, P. Liu, S. Zhang, *Chem. Commun.*, 2010, **46**, 1323–1325.
31. X. Yu, H. Xia, Z. Sun, Y. Lin, K. Wang, J. Yu, H. Tang, D. Pang, Z. Zhang, *Bio. Bio.*, 2013, **41**, 129–136.
32. D. Tang, R. Yuan, Y. Chai, *Anal. Chem.*, 2008, **80**, 1582–1588.
33. Z. Fu, Z. Yang, J. Tang, H. Liu, F. Yan, H. Ju, *Anal. Chem.*, 2007, **79**, 7376–7382.